Soil Moisture Estimation by Combining L-Band Brightness Temperature and Vegetation Related Information

Yuanyuan Fu, Chunjiang Zhao, Guijun Yang, Haikuan Feng

Soil moisture estimation by combining L-band brightness temperature and vegetation related information

Yuanyuan Fu[1, 2, 3], Chunjiang Zhao[1, 2, 3(✉)], Guijun Yang[1, 2, 3], Haikuan Feng[1, 2, 3]

[1]Key Laboratory of Quantitative Remote Sensing in Agriculture of Ministry of Agriculture P. R. China, Beijing Research Center for Information Technology in Agriculture, Beijing 100097, China .
{fuyy, zhaocj, yanggj, fenghk}@nercita.org.cn
[2]National Engineering Research Center for Information Technology in Agriculture, Beijing 100097, China
[3]Beijing Engineering Research Center for Agriculture Internet of Things, Beijing 100097, China

Abstract. Passive radiometry at L-band has been widely accepted as one of the most promising techniques for monitoring soil moisture content (SMC). However, with vegetation cover, the scatter and attenuation of microwave signals by vegetation make the discrimination of SMC related signal complicated. To improve SMC estimate, this study proposed the combined use of L-band brightness temperature (T_B) and optical remote sensing data to take into account the effect of vegetation. The normalized difference infrared index (NDII) and enhanced vegetation index (EVI) were used as proxy for including the effect of vegetation water content and structure. Considering viewing angle effects, T_B data were normalized to three different angles (7°, 21.5°, and 38.5°). The model based on the combination of NDII and horizontally polarized T_B normalized to 7° produced the best result (R^2=0.678, RMSE=0.026 m^3/m^3). It suggests that involving NDII into the model could significantly improve pasture covered SMC estimation accuracy.

Keywords: Soil moisture; L-band brightness temperature; vegetation water content; normalized difference infrared index; leaf area index; enhanced vegetation index

1. Introduction

Soil moisture is a critical factor in many land applications such as hydrology [1], flood forecasting [2], and precision agriculture [3]. Therefore, it is important to get reliable information on the spatio-temporal variations of near-surface soil moisture. Soil moisture estimates are traditionally based on contact-based methods that measure the electrical resistivity, or on gravimetric methods that measure the volume of water. But these point measurements are time-consuming and often not applicable to large areas [4]. Microwave remote sensing methods including passive microwave radiometer and active microwave (radar) deployed on either airborne or spaceborne platforms offer an effective way for retrieving spatial soil moisture estimates at different scales. In the past decades, passive microwave radiometer data have shown their increasing potential for quantifying and monitoring soil moisture [5, 6, 7, 8]. Particularly, L-band brightness temperature (T_B) has been widely accepted as one of the most promising techniques for quantifying soil moisture. A number of field experiments have demonstrated that L-band T_B has high sensitivity to moisture status and has a nearly linear relationship with near-surface soil moisture, providing that vegetation conditions or soil characters are uniform [9, 10, 11, 12]. In addition, L-band has been utilized and dedicated to Soil Moisture and Ocean Salinity (SMOS) mission [13], and NASA's Soil Moisture Active /Passive (SMAP) mission [14].

Although passive microwave radiation at L-band can penetrate vegetation canopies to a certain extent, the difficulty in estimating soil moisture significantly increases in the presence of vegetation. The main reason is that vegetation canopies can scatter and attenuate microwave radiation from soil surface, and also emit their own energy, so the signal received is modified such that the discriminate component of the signal due to soil moisture becomes complex [15, 16]. Therefore, the effects of vegetation must be taken into account when retrieving soil moisture with vegetation cover. Wigneron et al. [15] pointed out that the effects of vegetation can be well approximated by a simple radiative transfer model based on the optical depth, which could be derived from vegetation indices. The study of Wang et al. [16] showed that deseasonalized time series of root-zone soil moisture and normalized difference vegetation index (NDVI) have a nearly linear relationship. Pause et al. [4] reported that soil moisture estimation was improved by combining airborne L-band T_B observations with leaf area index (LAI) retrieved from hyperspectral image data. Cho et al. [17] found that the relationship between enhanced vegetation index (EVI) and soil moisture is nearly linear as a function of the

fraction of vegetation cover. The aforementioned studies all demonstrated that vegetation related information has a considerable correlation to soil moisture. However the combination of L-band T_B with vegetation related information, such as vegetation structure and vegetation water content (VWC), have not been quantitatively investigated for soil moisture retrieval. Thus, the objectives of this study are to (1) determine whether a multivariate linear model based on a combination of L-band T_B and vegetation structure related vegetation index could increase estimation accuracy; and (2) demonstrate if soil moisture estimation accuracy could be improved by combining L-band T_B with vegetation water content. We tested the use of normalized difference infrared index (NDII) and EVI, which were calculated from Landsat 5 Thematic Mapper (TM) images, to represent VWC and vegetation structure, respectively.

2. Data Sources

2.1. Ground Sampling Data from SMAPEx-3

The study site and data sets of the third Soil Moisture Active Passive Experiment (SMAPEx-3) [18] were used in this study. The SMAPEx-3 was undertaken in the Yanco area (145°50′ to 146°21′ E, 34°40′ to 35°0′ S) located in the western plains of the Murrumbidgee Catchment, Australia. The topography of the study area is flat with altitude no more than 150 m. This region is characterized by semi-arid agricultural and grazing area. The analyses in this study were mainly based on sampling data from three grazing areas. The three-week long campaign was conducted from September 5th to September 23rd, 2011.

The near surface (0-5 cm) soil moisture measurements were acquired along 250 m spaced regular grids using the Hydra-probe Data Acquisition System (HDAS) [19] for each flight day. To improve the accuracy and efficiency of ground sampling, a measurement grid was uploaded on the HDAS screen. Three replicate measurements were taken at each predefined sampling location and then averaged to account for small-scale soil moisture variation. Because the spatial resolution of L-band T_B data was 1 km, the average value of about 16 soil moisture measurements was used to represent soil moisture of a 1 km × 1 km grid. Thus, a total of 32 soil moisture measurements were obtained. Coincident with soil moisture sampling activities, the vegetation samples for LAI and VWC were also collected in the corresponding area. LAI observations were obtained by an LAI-2000 Plant Canopy Analyzer. At each location, an approximate 0.25 m^2 area of vegetation within the area was clipped at ground level and then sent to laboratory for VWC measurements. The detailed sampling protocol was further described in Panciera et al. [18].

2.2. L-band T_B Data

L-band T_B was measured at two polarizations using the Polarimetric L-band Multi-beam Radiometer (PLMR) deployed on a light aircraft. The PLMR observes at both horizontal and vertical polarization using a polarization switch, with viewing angles of ±7°, ±21.5° and ±38.5°. A footprint size of nearly 1 km was achieved with a flying altitude of 3 km. The details of before and after flight calibrations, radiometric calibration and final geo-rectification can be found in Monerris et al. [20]. The output data were time sequential datasets of six beam position T_B values with geo-reference for each flight line. The T_B data collected on September 5th, September 18th, September 19th and September 21th, 2011 were used in the study for analyses.

To effectively use T_B data for retrieving soil moisture, the varying viewing angles should be taken into account through a normalization procedure [21]. For this study, the data were normalized to 7°, 21.5° and 38.5°, respectively, to evaluate the influence of viewing angle on soil moisture retrieval. Taking the normalized horizontal polarization T_B to 7°, for example, a correction factor was first computed for each beam position (BP) by deducting its mean from the average value of BP 3 and BP 4, and then this factor was added to all data point for that BP. The processed and geo-referenced T_B values were mapped at a resolution of 1 km. Fig. 1 presents the maps of L-band T_B normalized to 7° in horizontal and vertical polarization acquired on September 5th, 2011.

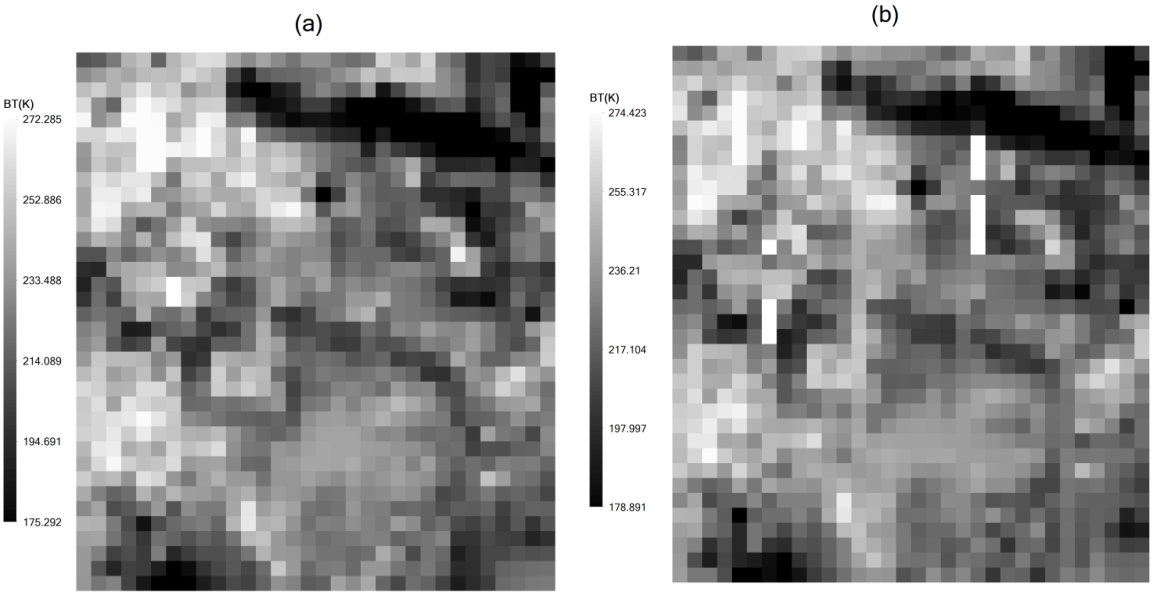

Fig.1. Example of L-band T_B normalized to 7° in horizontal (a) and vertical (b) polarization acquired on September 5th, 2011.

Due to the relatively low flying height, atmospheric contribution on L-band T_B could be neglected. Consequently, the T_B data were normalized and divided by the ground measured soil temperature (Ts) to remove difference in observed T_B due to seasonal Ts changes.

2.3. Landsat 5 Thematic Mapper Data

Two images of clear sky Landsat 5 TM, acquired on September 2nd and September 18th, 2011, were used in this study. These two images provided concurrent measurements during the SMAPEx-3 campaign. Because the changes in vegetation (biomass, VWC and vegetation structure) are negligible within a week, a time shift of two or three days to the L-band T_B data acquisition could be acceptable. TM surface reflectance values were obtained by applying the atmospheric correction algorithm in ENVI FLAASH.

3. Methods

3.1. Using Enhanced Vegetation Index as an Indicator of Vegetation Structure

LAI is an important vegetation structure parameter and is commonly estimated by vegetation indices. According to the existing research, EVI has widely accepted as one of optimal vegetation indices for LAI retrieval due to its capability in reducing atmospheric and soil interference [22, 23]. Through the statistical analysis of pasture LAI, most of the LAI values from SMAPEx-3 fell into the interval of [0, 3]. Because the relationship between LAI and EVI is nearly linear when LAI is less than three [24, 25], EVI is used as a proxy of LAI in this study and can be computed according to Eq. (1).

$$EVI = 2.5\frac{R_{NIR}-R_R}{R_{NIR}+6R_R-7.5R_B+1} \quad (1)$$

where R_{NIR} , R_R and R_B represent the reflectance of near-infrared channel (780-900 nm),red channel (630-690 nm) and blue channel (450-520 nm), respectively.

3.2. Using Normalized Difference Infrared Index as an Indicator of VWC

Many studies [26, 27, 28] have explored the utility of Landsat TM images in retrieving VWC. It has been found that NDII is the most appropriate index for VWC retrieval using Landsat TM images. Therefore, NDII is utilized as a proxy of VWC in this study since the relationship between NDII and VWC is approximately linear [29, 30]. The NDII could be calculated according to Eq. (2).

$$NDII = \frac{R_{NIR}-R_{SWIR}}{R_{NIR}+R_{SWIR}} \quad (2)$$

where R_{NIR} and R_{SWIR} represent the reflectance of near-infrared channel (780-900 nm) and shortwave infrared channel (1550-1750 nm), respectively.

3.3. Image Registration

To determine whether involving TM vegetation data can reduce the effect of vegetation on microwave signal and improve soil estimation accuracy, horizontal polarization and vertical polarization L-band T_B data normalized to three different viewing angles were respectively combined with NDII and EVI in turn for soil moisture estimation. Because T_B data and vegetation data derived from Landsat 5 TM imageries have different spatial resolution, it is necessary to resample the EVI and NDII maps of 30 m x 30 m to 1 km × 1 km pixel. EVI and NDII maps were down-sampled using the nearest neighbor interpolation algorithm in this study.

3.4. Multivariate Linear Regression Modelling

The previous studies demonstrated that the relationship between L-band T_B and soil moisture is nearly linear (Merlin et al., 2008; Panciera et al., 2014), and the relationship between vegetation related data and soil moisture is also approximately linear [16, 17]. Therefore, a multivariate linear regression model was adopted in this study to estimate soil moisture as a weighted sum of L-band T_B data and a vegetation related measurement. The model is trained as

$$\boldsymbol{Y} = \boldsymbol{X}\beta + \varepsilon \tag{3}$$

where the dependent variable $\boldsymbol{Y}$ is an n × 1 vector for the soil moisture content with n being the number of training samples; the independent variable $\boldsymbol{X}$ is an n × 2 matrix of the two observed values for each training sample. One observed value is the T_B of a given viewing angle under a given polarization, and the other is the vegetation information (NDII or EVI). The β is a 2 × 1 vector of regression coefficients and ε is an n × 1 vector of residuals. The regression coefficients were obtained by minimizing a least square cost function of Eq. (3). Three viewing angles under two polarizations were tested by applying the multivariate regression model with T_B and NDII, or with T_B and EVI.

3.5. Validation

Due to the limited number of samples in this study, leave-one-out cross validation (LOOCV) was utilized to assess the overall performance of different models. This meant that 32 individual calibration models were developed for each method. The average coefficient of determination (R^2_{avg}) and average root mean square error ($RMSE_{avg}$) of 32 calibration models were used to evaluate the calibration accuracy. The coefficient of determination for LOOCV (R^2_{cv}) and root mean square error for LOOCV ($RMSE_{cv}$) were selected to further compare the performances of various models. The proposed models T_B +EVI and T_B +NDII were compared with the case of using T_B only for three viewing angles of two polarizations.

4. Results

4.1. Multivariate Linear Regression Using the Combination of T_B and EVI

Table 1 gives the comparison results on the performance of the multivariate linear regression models. It shows that T_B+EVI produced little better (or similar) results than those with the T_B only for both calibration and LOOCV analyses. In the multivariate linear regression analyses, models involving horizontal (H) polarization T_B performed considerably better than those involving vertical (V) polarization T_B. Of them, the model based on the combination of EVI and horizontal polarization T_B normalized to 7° yielded the best results for both calibration (R^2_{avg}=0.686, $RMSE_{avg}$=0.026 m^3/m^3) and validation (R^2_{cv}=0.572, $RMSE_{cv}$=0.029 m^3/m^3). The followed were models involving horizontal polarization T_B normalized to 38.5°. The models involving horizontal polarization T_B normalized to 21.5° performed the worst.

Table 1 Performance of the multivariate linear regression models based on the combination of L-band T_B and EVI for predicting soil moisture.

	Calibration		Validation	
	R^2_{avg}	$RMSE_{avg}$ (m^3/m^3)	R^2_{cv}	$RMSE_{cv}$ (m^3/m^3)
7°				

T_B(H)	0.641	0.028	0.579	0.030
T_B(H)+EVI	0.686	0.026	0.572	0.029
T_B(V)	0.594	0.030	0.516	0.032
T_B(V)+EVI	0.623	0.028	0.502	0.032
21.5°				
T_B(H)	0.607	0.029	0.545	0.031
T_B(H)+EVI	0.640	0.028	0.541	0.031
T_B(V)	0.542	0.032	0.451	0.034
T_B(V)+EVI	0.583	0.030	0.453	0.033
38.5°				
T_B(H)	0.624	0.029	0.559	0.031
T_B(H)+EVI	0.674	0.026	0.559	0.030
T_B(V)	0.423	0.035	0.310	0.038
T_B(V)+EVI	0.500	0.032	0.356	0.036

4.2. Multivariate Linear Regression Using the Combination of T_B and NDII

Table 2 gives comparison results on the performance of the multivariate linear regression models based on the combination of L-band T_B and NDII for predicting soil moisture. This model produced generally better results than those with the T_B only, for both calibration and LOOCV analyses. In the multivariate linear regression analyses, models involving horizontal polarization T_B values performed considerably better than those involving vertical polarization T_B values. Among these models, the performances of models involving horizontal polarization T_B normalized to 7° were the best. Especially, the model based on the combination of horizontal polarization T_B and NDII resulted in the highest estimation accuracy with R^2_{cv}=0.678, $RMSE_{cv}$=0.026 m^3/m^3. The models involving horizontal polarization T_B normalized to 38.5° produced almost similar estimation accuracy to those involving horizontal polarization T_B normalized to 7°. The followed were models involving horizontal polarization T_B normalized to 21.5°.

Table 2 Performance of the multivariate linear regression models based on the combination of L-band T_B and NDII for predicting soil moisture.

	Calibration		Validation	
	R^2_{avg}	$RMSE_{avg}$ (m^3/m^3)	R^2_{cv}	$RMSE_{cv}$ (m^3/m^3)
7°				
T_B(H)	0.641	0.028	0.579	0.030
T_B(H)+NDII	0.746	0.023	0.678	0.026
T_B(V)	0.594	0.030	0.516	0.032
T_B(V)+NDII	0.692	0.025	0.614	0.028
21.5°				
T_B(H)	0.607	0.029	0.545	0.031
T_B(H)+NDII	0.711	0.025	0.641	0.027
T_B(V)	0.542	0.032	0.451	0.034
T_B(V)+NDII	0.658	0.027	0.568	0.030
38.5°				
T_B(H)	0.624	0.029	0.559	0.031
T_B(H)+NDII	0.742	0.023	0.673	0.026
T_B(V)	0.423	0.035	0.310	0.038
T_B(V)+NDII	0.598	0.029	0.491	0.032

Fig. 2(a) shows the relationship between the modeled results and the ground truth, when only T_B (H) 7° was used. Fig. 2(b) shows the performance after NDII was added. In the comparison of Fig. 2 (a) and Fig. 2 (b), it can be observed that linear relationship between the measured soil moisture and the predicted soil moisture was significantly improved. This model increased R^2_{cv} value by 0.099, and

decreased the $RMSE_{cv}$ value by 0.004 m^3/m^3 in the cross-validation after involving NDII.

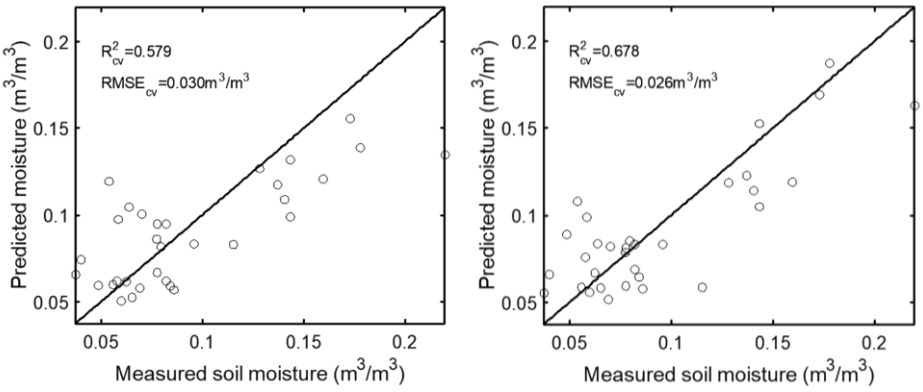

(a) (b)

Fig.2. LOOCV results before (a) and after (b) involving NDII for predicting soil moisture using horizontal polarization L-band T_B normalized to 7°. Note: The solid line is a one-to-one line.

5. Discussion and Conclusions

The SMAPEx-3 led to reliable passive radiometry data at L-band and corresponding ground sampling data including soil moisture and vegetation data. It allowed an assessment of the utility of passive radiometry data at L-band for use in estimating soil moisture below pasture. It also made it possible to explore whether soil moisture estimation could be enhanced by involving vegetation related information.

The performance of multivariate linear regression models involving vegetation structure related information (LAI) was little better than those with only T_B under three viewing angles (Table 1). These results are not consistent with that observed in Pause et al. [4] who found that soil moisture estimation accuracy was significantly improved after combining L-band T_B and LAI. This study retrieved winter barley covered and winter rye covered soil moisture using horizontal polarization T_B data with 50 m spatial resolution and LAI estimated from hyperspectral data with 1.5 m spatial resolution. The primary reason is that hyperspectral data are more powerful than multispectral data for LAI estimation due to its approximately contiguous spectrum [31]. Furthermore, the best pasture LAI estimation accuracy got by EVI was relatively low (R^2_{cv}=0.385, $RMSE_{cv}$=0.75 m^2/m^2) based on Landsat 5 TM data in the study (the detailed comparison was not presented in this paper). It demonstrated that LAI estimation accuracy based on remote sensed data should be checked before involving LAI into soil moisture estimation. If LAI estimation is not accurate, it will not work to involve it during soil moisture estimation.

The models involving horizontal polarization T_B values performed better than those involving vertical polarization T_B values (Table 1 and Table 2). It indicated that horizontal polarization T_B was more sensitive to soil moisture than vertical polarization T_B. Many researchers [4, 18] have given the same conclusion about this. The performances of multivariate linear regression models involving NDII were much better than those with only T_B at both polarizations under three different viewing angles. This is mainly due to the fact that involving NDII takes VWC into account and relieves the effect of vegetation on microwave signal. Among the three viewing angles, models based on T_B normalized to 7° or 38.5° resulted in better estimation accuracy than those based on T_B normalized to 21.5° with and without NDII. It confirmed that effects of vegetation and soil moisture estimation based on microwave signal are dependent on incidence angle.

In summary, this study demonstrated the potential application of involving vegetation related information into soil moisture estimation. The experimental results indicated that multivariate linear regression models using horizontal polarization T_B and NDII could significantly improve pasture covered soil moisture estimation accuracy. It is also worth mentioning that this newly developed method based on empirical models might be site-specific and thus needs recalibrating or testing the models with a certain amount of samples collected from an application area before applying the method to the area. It is necessary to do further study to verify the efficacy of the proposed method in different vegetation types and under different ecological areas.

Acknowledgements

This study was supported by the National Key Research and Development Program (2016YFD0300602), Natural Science Foundation of China (61661136003, 41601346, 41471285, 41471351, 41371349), China Postdoctoral Science Foundation Funded Project (2017M620675), the Special Funds for Technology innovation capacity building sponsored by the Beijing Academy of Agriculture and Forestry Sciences (KJCX20170423) and Beijing Postdoctoral Research Foundation. The authors wish to thank Xiuping Jia at University of New South Wales at Canberra, Jeffrey P. Walker and Xiaoling Wu at Monash University for providing comments and experimental data.

References

1. Crow, W. T., Chen, F., Reichle, R. H., et al.: L-band microwave remote sensing and land data assimilation improve the representation of pre-storm soil moisture conditions for hydrologic forecasting. Geophysical Research Letters, (2017)
2. Meng, S., Xie, X., Liang, S.: Assimilation of soil moisture and streamflow observations to improve flood forecasting with considering runoff routing lags. Journal of hydrology, 550, 568-579 (2017)
3. Tian, L., Yuan, S., Quiring, S. M.: Evaluation of six indices for monitoring agricultural drought in the south-central United States. Agricultural and Forest Meteorology, 249, 107-119 (2018)
4. Pause, M., Schulz, K., Zacharias, S., et al.: Near-surface soil moisture estimation by combining airborne L-band brightness temperature observations and imaging hyperspectral data at the field scale. Journal of Applied Remote Sensing, 6, 063516-1(2012)
5. Wigneron, J. P., Jackson, T. J., O'neill, P., et al.: Modelling the passive microwave signature from land surfaces: A review of recent results and application to the L-band SMOS SMAP soil moisture retrieval algorithms. Remote Sensing of Environment, 192, 238-262. (2017)
6. Kolassa, J., Reichle, R. H., Draper, C. S.: Merging active and passive microwave observations in soil moisture data assimilation. Remote sensing of environment, 191, 117-130 (2017)
7. Chan, S. K., Bindlish, R., O'Neill, P. E., et al.: Assessment of the SMAP passive soil moisture product. IEEE Transactions on Geoscience and Remote Sensing, 54(8), 4994-5007 (2016)
8. Santi, E., Paloscia, S., Pettinato, S., et al.: Application of artificial neural networks for the soil moisture retrieval from active and passive microwave spaceborne sensors. International journal of applied earth observation and geoinformation, 48, 61-73(2016)
9. Merlin, O., Walker, J. P., Kalma, J. D., et al.: The NAFE'06 data set: Towards soil moisture retrieval at intermediate resolution. Advances in Water Resources, 31, 1444-1455 (2008)
10. Colliander, A., Jackson, T., McNairn, H., et al.: Comparison of airborne passive and active L-band system (PALS) brightness temperature measurements to SMOS observations during the SMAP validation experiment 2012 (SMAPVEX12). IEEE Geoscience and Remote Sensing Letters, 12(4), 801-805(2015)
11. Fernandez-Moran, R., Wigneron, J. P., Lopez-Baeza, E., et al.: Roughness and vegetation parameterizations at L-band for soil moisture retrievals over a vineyard field. Remote Sensing of Environment, 170, 269-279 (2015)
12. Chen, X., Su, Y., Liao, J., et al.: Detecting significant decreasing trends of land surface soil moisture in eastern China during the past three decades (1979–2010). Journal of Geophysical Research: Atmospheres, 121(10), 5177-5192 (2016)
13. Kerr, Y. H., Waldteufel, P., Wigneron, J. P., et al.: Soil moisture retrieval from space: The Soil Moisture and Ocean Salinity (SMOS) mission. IEEE Transactions on Geoscience and Remote Sensing. 39, 1729-1735 (2001)
14. Entekhabi, D., Njoku, E. G., O'Neill, P. E., et al.: The soil moisture active passive (SMAP) mission. Proceedings of the IEEE, 98(5), 704-716 (2010)
15. Wigneron, J. P., Kerr, Y., Waldteufel, P., et al.: L-band microwave emission of the biosphere (L-MEB) model: Description and calibration against experimental data sets over crop fields. Remote Sensing of Environment, 107(4), 639-655 (2007)
16. Wang, X., Xie, H., Guan, H., et al.: Different responses of MODIS-derived NDVI to root-zone soil moisture in semi-arid and humid regions. Journal of Hydrology, 340, 12-24(2007)
17. Cho, J., Lee, Y. W., Han, K. S.: The effect of fractional vegetation cover on the relationship between EVI and soil moisture in non-forest regions. Remote Sensing Letters, 5, 37-45 (2014)
18. Panciera, R., Walker, J. P., Jackson, T. J., et al.: The soil moisture active passive experiments (SMAPEx): Toward soil moisture retrieval from the SMAP mission. IEEE Transactions on Geoscience and Remote Sensing, 52, 490-507(2014)
19. Merlin, O., Walker, J., Panciera, R., et al.: Soil moisture measurement in heterogeneous terrain. Proc. Int. Congr. MODSIM, 10-13 (2007)
20. Monerris, A., Walker, J. P., Panciera, R., et al.: The third soil moisture active passive experiment. In The 19th International Congress on Modeling and Simulation (MODSIM2011). Modelling and Simulation Society of Australia and New Zealand, 1980-1986 (2011)
21. Jackson, T. J., Le Vine, D. M., Swift, C. T., et al.: Large area mapping of soil moisture using the ESTAR passive microwave radiometer in Washita'92. Remote Sensing of Environment, 54, 27-37 (1995)

22. Jiang, Z., Huete, A. R., Didan, K., et al.: Development of a two-band enhanced vegetation index without a blue band. Remote sensing of Environment, 112(10), 3833-3845 (2008)
23. Thenkabail, P. S., Lyon, J. G. (Eds.). Hyperspectral remote sensing of vegetation. CRC Press (2016)
24. Fu, Y., Yang, G., Wang, J., et al.: A comparative analysis of spectral vegetation indices to estimate crop leaf area index. Intelligent Automation Soft Computing, 19(3), 315-326 (2013)
25. Wu, M., Wu, C., Huang, W., et al.: High-resolution Leaf Area Index estimation from synthetic Landsat data generated by a spatial and temporal data fusion model. Computers and electronics in agriculture, 115, 1-11(2015)
26. Trombetti, M., Riaño, D., Rubio, M. A., et al.: Multi-temporal vegetation canopy water content retrieval and interpretation using artificial neural networks for the continental USA. Remote Sensing of Environment, 112(1), 203-215(2008)
27. Adam, E., Mutanga, O., Rugege, D.: Multispectral and hyperspectral remote sensing for identification and mapping of wetland vegetation: a review. Wetlands Ecology and Management, 18(3), 281-296 (2010)
28. Gao, Y., Walker, J. P., Allahmoradi, M., et al.: Optical sensing of vegetation water content: A synthesis study. IEEE Journal of Selected Topics in Applied Earth Observations and Remote Sensing, 8(4), 1456-1464 (2015)
29. Cosh, M. H., Tao, J., Jackson, T. J., et al.: Vegetation water content mapping in a diverse agricultural landscape: National Airborne Field Experiment 2006. Journal of Applied Remote Sensing, 4, 043532-043532(2010)
30. Xiao, Y., Zhao, W., Zhou, D., et al.: Sensitivity analysis of vegetation reflectance to biochemical and biophysical variables at leaf, canopy, and regional scales. IEEE Transactions on Geoscience and Remote Sensing, 52(7), 4014-4024 (2014)
31. Xing, J., Symons, S., Shahin, M., et al.: Detection of sprout damage in Canada Western Red Spring wheat with multiple wavebands using visible/near-infrared hyperspectral imaging. Biosystems Engineering, 106, 188-194 (2010)